Analysis and Improvement of Mach–Zehnder Modulator Linearity Performance for Chirped and Tunable Optical Carriers

S. Dubovitsky, *Member, IEEE,* W. H. Steier, *Life Fellow, IEEE,* S. Yegnanarayanan, and B. Jalali, *Senior Member, IEEE*

***Abstract*—Photonic systems that use a variable or chirped optical wavelength and a single Mach–Zehnder modulator have been analyzed to determine the relation between optical bandwidth and spur free dynamic range. A novel wavelength insensitive biasing technique is proposed which significantly reduces the second-order distortion and increases the optical bandwidth.**

***Index Terms*—Photonic assisted A/D, RF photonics, wavelength-division multiplexing.**

I. Introduction

THE WAVELENGTH response of a Mach–Zehnder (MZ) intensity modulator plays an important role in wavelength-division multiplexing (WDM) systems where a single variable wavelength or multiple fixed wavelengths may be modulated by a single modulator. The modulator properties relevant to WDM systems have been investigated [1]. Similar to WDM systems, modulator wavelength response plays a key role in photonic time stretch and WDM sampling techniques currently being investigated for enhancing the performance of analog-to-digital converters (ADC) [2]. In these systems, the carrier wavelength is continuously tuned while the modulation is being applied. Also, a dense WDM digital system has been demonstrated which uses a single modulator and a chirped laser to transmit a TDM signal over multiple wavelength channels [3].

Changes in the carrier wavelength shift the modulator bias from the optimum $\pi/2$ bias point and cause a strong increase in the second-order distortion. At a certain detuning from the center wavelength, the second-order distortion begins to exceed the third-order distortion. In systems with greater than one octave bandwidth, this begins to degrade the spur free dynamic range (SFDR) of the system. To prevent SFDR degradation due to second-order distortion, one therefore must limit the optical bandwidth of the system.

In this paper, we extend the modulator response analysis to systems with a chirped optical carrier and introduce a technique for second-order distortion suppression applicable to all multi-wavelength systems. This technique enables one to greatly extend the optical bandwidth of the system.

Manuscript received August 30, 2001; revised January 30, 2002. This work was supported in part by the Air Force Office of Scientific Research and the Defense Advanced Research Projects Agency under the COAST Program.

S. Dubovitsky and W. H. Steier are with the Department of Electrical Engineering, University of Southern California, Los Angeles, CA 90089-0483 USA (e-mail: dubovits@usc.edu).

S. Yegnanarayanan and B. Jalali are with the Department of Electrical Engineering, University of California, Los Angeles, CA 90089-0483 USA.

Publisher Item Identifier S 0733-8724(02)05120-4.

II. Basics and Single Wavelength Operation

The MZ modulator transmission as a function of applied voltage (V) is given by

$$T(\lambda) = \frac{1}{2}\left[1 + \cos\left(\pi \frac{V}{V_\pi(\lambda)} + \phi_b(\lambda)\right)\right] \tag{1}$$

where

$$\phi_b = 2\pi\frac{\Delta_{nL}}{\lambda} + \pi\frac{V_b}{V_\pi} \quad \text{is the modulator phase bias;} \tag{1a}$$

Δ_{nL} internal pathlength mismatch between the two arms of the interferometer, $n_1L_1 - n_2L_2$;
λ optical wavelength in vacuum;
V_b externally applied bias voltage;

$$V_\pi(\lambda) = \frac{\lambda d}{2\Gamma(\lambda)n^3(\lambda)r(\lambda)L_m}; \tag{1b}$$

d electrode separation;
L_m electrode length;
$\Gamma(\lambda)$ confinement factor which is defined as the ratio of the change in the effective index of refraction of the waveguide mode to the change in index of refraction of the electrooptic material;
$n(\lambda)$ index of refraction;
$r(\lambda)$ electrooptic coefficient.

We want to look at the first- and second-order intermodulation distortions and their impact on the SFDR. Kolner and Dolfi have derived in [4] the general expressions for the spectral components of the photodetector current assuming a two-tone signal. In the following, we assume that both tones have equal amplitudes (V):

$$\mathbf{i}_1 = -C_\mathbf{i} 2\sin\phi_b J_1\left(\pi\frac{V}{V_\pi}\right) J_o\left(\pi\frac{V}{V_\pi}\right)$$
is the signal current (2a)

$$\mathbf{i}_2 = -C_\mathbf{i} 2\cos\phi_b J_1^2\left(\pi\frac{V}{V_\pi}\right)$$
is the second-order intermodulation distortion (2b)

$$\mathbf{i}_3 = C_\mathbf{i} 2\sin\phi_b J_1\left(\pi\frac{V}{V_\pi}\right) J_2\left(\pi\frac{V}{V_\pi}\right)$$
is the third-order intermodulation distortion (2c)

where

C_i constant containing detector responsivity and optical power;

J_n Bessel function of the first kind of order n.

When the modulator is biased at $\phi_b = \pi/2$, the second-order distortion is eliminated. The SFDR is dominated by the third order and, assuming shot noise limit, is given in [4] by

$$\mathrm{SFDR_3\ (dB)} = \frac{20}{3}\log\left(\frac{2i_{\mathrm{ave}}}{qB}\right) \tag{3}$$

where

i_{ave} average current out of the photodetector;

B electrical bandwidth;

q electron charge.

As the wavelength detunes from the nominal, λ_o, two effects occur: the bias deviates from $\pi/2$ and the modulation index, $m \equiv \pi\frac{V}{V_\pi(\lambda)}$, changes because of changing V_π. The bias shift causes a very rapid increase in the second-order distortion, but has a small impact on the fundamental and third-order distortion terms [5] and, therefore, at some wavelength detuning, the system SFDR starts degrading due to the rising second-order intermodulation distortion. The second effect, change in the modulation index, has a much smaller effect on the system SFDR.

Consequently, it is the rise of the second-order distortion due to the bias shift that limits the optical bandwidth of the modulator. The change in phase bias away from $\pi/2$ at which the SFDR begins to be determined by the second order [4], assuming $\mathrm{SFDR_3} \gg 1$ and using (3) to solve for (qB/i_{ave}), is given by

$$\begin{aligned}\Delta\phi_b &= \phi_b - \frac{\pi}{2} \approx \pm 2^{-(2/3)}\left(\frac{qB}{i_{\mathrm{ave}}}\right)^{1/6} \\ &= \pm\frac{1}{\sqrt{2}}10^{-(\mathrm{SFDR_3})/40}.\end{aligned} \tag{4}$$

For an internally trimmed modulator that does not require bias voltage, i.e., $2\pi(\Delta_{nL}/\lambda) = \pi/2$, the allowable optical bandwidth is given by

$$\Delta\lambda = \frac{2\sqrt{2}}{\pi}10^{-(\mathrm{SFDR_3}/40\lambda_o)} \tag{5}$$

meaning that the wavelength can deviate by $\pm(1/2)\Delta\lambda$ from the center wavelength, λ_o, before the SFDR degrades below the specified value due to second-order distortion. For an SFDR of 80 dB at $\lambda_o = 1550$ nm, this distortion limits the optical bandwidth to $\Delta\lambda = 14$ nm.

If the modulator was biased at a higher multiple of $\pi/2$, then the wavelength dependence would be higher and the bandwidth appropriately lower.

For an untrimmed modulator that does require bias voltage, i.e., $2\pi(\Delta_{nL}/\lambda) = 0$ and $V_b = V_\pi/2$, the allowable optical bandwidth is given by

$$\Delta\lambda = \frac{2\sqrt{2}}{\pi}10^{-(\mathrm{SFDR_3}/40)}\frac{V_\pi(\lambda_o)}{dV_\pi/d\lambda|_{\lambda_o}}. \tag{6}$$

For a typical $LiNbO_3$ modulator [6] with $dV_\pi/d\lambda = 8$ V/μm and $V_\pi = 6.6$ V and, again assuming an SFDR of 80 dB, the optical bandwidth is limited to 7.4 nm.

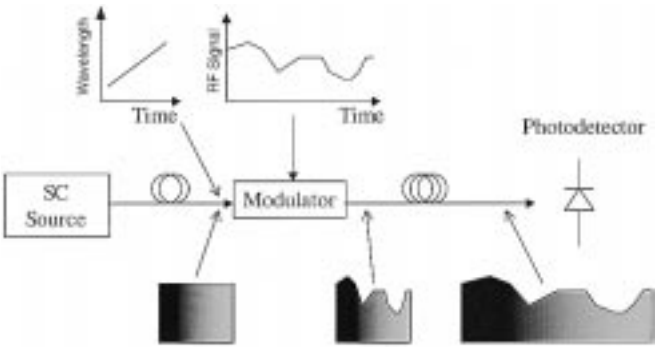

Fig. 1. Photonic time stretch system.

III. Chirped Carrier

In the photonic time stretch systems [2], illustrated in Fig. 1, a continuously swept wavelength (chirped carrier) is fed into the modulator. In this section, we extend the above analyses to determine the optical bandwidth limitations imposed on the chirped wavelength system by the wavelength dependent modulator response.

We need to look at the powers in various spectral harmonics generated at the output of the modulator. We have approached the problem in two ways. The proper way to do this with a continuously tunable wavelength is to combine the signal modulation and the additional modulation due to changing carrier wavelength over the time aperture of interest and then take a Fourier transform. This is how the results of our numerical simulations were obtained. To get the simplified analytical results, we used the expressions for harmonics amplitudes obtained for a single fixed wavelength, from (2), and averaged the power in these harmonics over the wavelength sweep. This is acceptable as long as the modulation induced by the temporal variation of the carrier wavelength is small. The simplified analytical treatment allows us to make predictions that are then compared with and confirmed by exact numerical simulations.

The RF power in the harmonics averaged over wavelength sweep $\Delta\lambda$ around center wavelength λ_o is given by

$$\overline{P}_j = C_P\frac{1}{\Delta\lambda}\int_{\lambda_o-(\Delta\lambda/2)}^{\lambda_o+(\Delta\lambda/2)}|\mathbf{i}_j(\lambda)|^2\,d\lambda \tag{7}$$

where $i_j(\lambda)$ are the photodetector currents given in (2) and $j = 1$ is the fundamental, $j = 2$ second-order, and $j = 3$ third-order intermodulation distortions. C_P is the constant to convert currents to relevant electrical powers.

The integration produces the following results:

$$\begin{aligned}\overline{P}_1 &= C_P 2J_1^2\left(\pi\frac{V}{V_\pi}\right)J_0^2\left(\pi\frac{V}{V_\pi}\right)[1+\mathrm{sinc}\,(\Delta\phi_{\mathrm{b}})] \\ \overline{P}_2 &= C_P 2J_1^4\left(\pi\frac{V}{V_\pi}\right)[1-\mathrm{sinc}\,(\Delta\phi_{\mathrm{b}})] \\ \overline{P}_3 &= C_P 2J_1^2\left(\pi\frac{V}{V_\pi}\right)J_2^2\left(\pi\frac{V}{V_\pi}\right)[1+\mathrm{sinc}\,(\Delta\phi_{\mathrm{b}})] \\ &\text{where } \Delta\phi_b \equiv \left.\frac{d\phi_b}{d\lambda}\right|_{\lambda_o}\Delta\lambda, \quad \mathrm{sinc}(x) = \frac{\sin(x)}{x}\end{aligned} \tag{8}$$

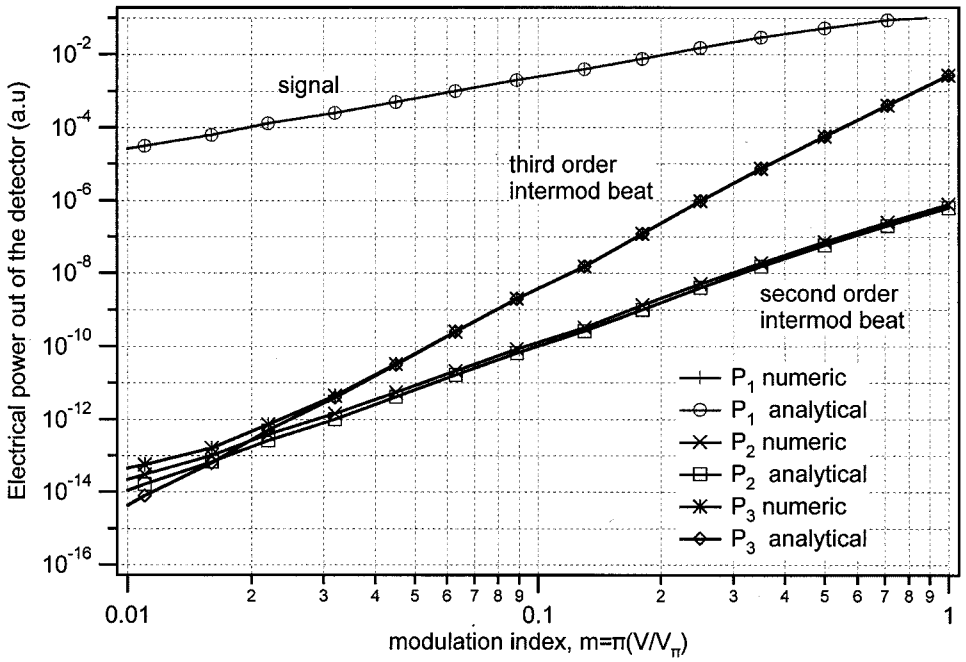

Fig. 2. Comparison of approximate analytical and exact numerical simulations for the chirped wavelength system. m_o is the modulation index at the center wavelength λ_o. The optical bandwidth is 14 nm. Simulation is performed over the time aperture equal to 1000 signal periods and there are about eight points per period.

The results predicted by these analytical equations are verified by exact numerical simulations and both are shown in Fig. 2.

The third-order-distortion-limited spur free dynamic range, SFDR_3, remains unchanged by the swept wavelength operation and is still given by (3)

$$\mathrm{SFDR}_3(\mathrm{dB}) = \frac{20}{3}\log\left(\frac{2i_{\mathrm{ave}}}{qB}\right). \tag{9}$$

This occurs because the fundamental and third-order terms are impacted similarly by the bias shift due to changing wavelength.

The phase bias deviation away from $\pi/2$ during the wavelength sweep at which the SFDR begins to be determined by the second-order distortions is now given by

$$\Delta\phi_b = \pm\sqrt{3}2^{(1/3)}\left(\frac{qB}{i_{\mathrm{ave}}}\right)^{1/6} = \pm\sqrt{6}10^{-(\mathrm{SFDR}_3/40)} \tag{10}$$

and is different from the single tunable wavelength case only by a small constant. For an internally trimmed modulator that does not require bias voltage, the allowable optical bandwidth is now given by

$$\Delta\lambda = \frac{2\sqrt{6}}{\pi}10^{-(\mathrm{SFDR}_3/40)}\lambda_o. \tag{11}$$

For an SFDR of 80 dB at $\lambda_o = 1550$ nm, this distortion limits the optical bandwidth to $\Delta\lambda = 24.2$ nm.

For an untrimmed modulator that does require bias voltage, i.e., $2\pi(\Delta_{nL}/\lambda) = 0$ and $V_b = V_\pi/2$, the allowable optical bandwidth is given by

$$\Delta\lambda = \frac{2\sqrt{6}}{\pi}10^{-\mathrm{SFDR}_3/40}\frac{V_\pi(\lambda_o)}{dV_\pi/d\lambda|_{\lambda_o}}. \tag{12}$$

Again using a typical $LiNbO_3$ modulator numbers [6]: $(dV_\pi/d\lambda) = 8$ V/μm and $V_\pi = 6.6$ V and assuming an SFDR of 80 dB; the optical bandwidth is limited to $\Delta\lambda$ =13 nm.

The chirped wavelength and single tunable wavelength cases behave differently, because in the chirped wavelength case the effects are averaged over all the wavelengths within the sweep; whereas, in the single tunable wavelength case the bias change is due to single maximally detuned wavelength.

IV. Suppression of the Second-Order Distortion: Wavelength Insensitive Bias Technique

In the above sections, we discussed how a typical modulator limits the optical bandwidth of the system. For an 80-dB SFDR, the allowable optical bandwidth is limited to 14 or 24 nm. The limitation of the allowable optical bandwidth may limit the performance of the photonic time stretch systems, because for a given stretch factor and fiber loss budget the time aperture of the system is directly proportional to the optical bandwidth. [2]. It is, therefore, highly desirable to use the entire width of the optical spectrum available from the supercontinuum sources (>60 nm). In this section, we introduce a technique that can greatly extend the optical bandwidth of the modulator. The wavelength insensitive bias (WIB) technique suppresses the bias point dependence on wavelength by adjusting various components of bias dependence to counterbalance each other.

The bias of the modulator is given by (1a), which is repeated here for convenience

$$\phi_b = 2\pi\frac{\Delta_{nL}}{\lambda} + \pi\frac{V_b}{V_\pi} \tag{13}$$

where V_b is the bias voltage used to trim the modulator and Δ_{nL} is the pathlength mismatch between the two arms of the MZ modulator.

We want to arrange it so that 1) at the center wavelength, λ_o, the modulator is biased at $\pi/2$ and 2) the bias does not change, to the first order, as the wavelength detunes from the center:

Condition 1)

$$\phi_b = \pi/2 \text{ at } \lambda_o \text{ and} \tag{14}$$

Condition 2)

$$\left.\frac{d\phi_b}{d\lambda}\right|_{\lambda_o} = 0. \tag{15}$$

Condition 1) implies the following connection between the internal modulator pathlength mismatch and the required bias voltage:

$$V_b = \frac{V_{\pi o}}{2}\left[1 - 4\frac{\Delta_{nLo}}{\lambda_o}\right] \tag{16}$$

where $V_{\pi o} = V_\pi(\lambda_o)$, i.e., $V\pi$ at the center of the wavelength sweep and condition 2) results in the following choice for internal pathlength mismatch

$$\Delta_{nLo} = \frac{\lambda}{4}\left[\frac{R - 4\frac{d\Delta_{nL}}{d\lambda}}{R-1}\right] \tag{17}$$

where

$$R \equiv \frac{\left.\frac{dV_\pi}{d\lambda}\right|_{\lambda_o}}{\frac{V_{\pi o}}{\lambda_o}}.$$

In the above equation, the ratio R expresses the nonlinearity of the V_π dependence on wavelength and is a key characteristic of the modulator. It can be thought of as a ratio of a local slope of the V_π dependence on wavelength, $dV_\pi/d\lambda|_{\lambda_o}$, to the slope of the global linear approximation, $V_{\pi o}/\lambda_o$.

The expression for V_π is given in (1b) and it can be seen that if the confinement factor (Γ), index (n), and r were wavelength independent, then V_π would be a linear function of wavelength and the ratio R would be equal to one. This in turn would drive the denominator to zero indicating that there is no finite internal pathlength mismatch, Δ_{nLo}, which would make the modulator bias insensitive to wavelength. Fortunately, this turns out not to be the case for typical modulators.

For example, a polymer modulator built at USC has a $V_\pi = 1.2$ V at 1.310 μm and $V_\pi = 1.8$ V at 1.550 μm [7] resulting in $dV_\pi/d\lambda = 2.5$ V/μm. At 1.55 μm, this gives $R = 2.2$ indicating that it is possible to calculate finite optimum Δ_{nL} and use the WIB technique.

The term $4(d\Delta_{nL}/d\lambda)$ expresses the change in internal pathlength mismatch with wavelength. This occurs due to index change with wavelength and is much smaller than R. For example, for a polymer modulator $dn/d\lambda \approx -0.02\ \mu\text{m}^{-1}$ at 1.55 μm. Assuming an ideal pathlength mismatch of $\Delta_{nL} = \lambda/4$ and an index of $n \sim 1.6$, we have a length mismatch of $\Delta L = 242$ nm resulting in

$$4\frac{d\Delta_{nL}}{d\lambda} = 4\frac{dn}{d\lambda}\Delta L = 0.02. \tag{18}$$

Because the value of $4(d\Delta_{nL}/d\lambda) \sim 0.02$ is much smaller than $R \sim 2$, it can be neglected in (17) resulting in a simple prescription for an internal modulator pathlength mismatch that, for a given modulator, eliminates the first-order dependence of bias point on carrier wavelength

$$\Delta_{nLo} \approx \frac{\lambda}{4}\left[\frac{R}{R-1}\right]. \tag{19}$$

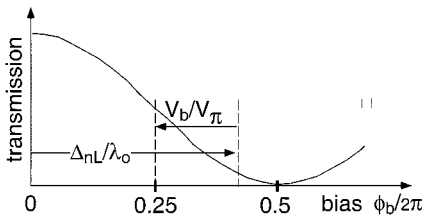

Fig. 3. Illustration of the WIB technique. The modulator is biased away from quadrature with an internal pathlength mismatch, but then external bias voltage is used to trim the bias back to quadrature. With an appropriate choice of Δ_{nL} and V_b wavelength dependent bias drift is eliminated to first order.

For the polymer modulator considered above with $R = 2.2$, we get $\Delta_{nLo} = 0.46\,\lambda$. Consequently, if we adjust the internal pathlength mismatch of the referenced modulator to 0.46 λ and use bias voltage equal to $V_b = -0.42\,V_\pi$ to trim the phase bias to $\pi/2$, as shown in Fig. 3, then the first-order dependence of the phase bias on wavelength will be eliminated. This occurs because the effect on phase bias of V_π changing with wavelength cancels the phase bias changes due to wavelength dependence of the internal bias.

Fig. 4 shows the numerical simulation of modulation spectra coming out of (a) modulator with an internal pathlength bias of $\lambda/4$ and (b) polymer modulator biased using a WIB technique. In the WIB modulator additional internal pathlength offset is used to match the V_π wavelength dependence and the second-order distortion is suppressed by 24 dB. At this point, we are able to calculate the improvement afforded by the WIB technique, but are unable to determine the ultimate optical spectrum allowed by the technique, because the performance-limiting residual second-order distortion is due to higher order dependencies of V_π on wavelength. To calculate the resulting allowable optical spectrum for a WIB modulator, one would have to determine and consider these higher order V_π dependencies. This issue is not part of this paper and may be considered in a later publication.

V. WIB Technique Implementation Issues and Tolerances

In this section, we identify the modulator properties needed to enable the WIB technique and consider manufacturing tolerances.

Equation (19) specifies the internal pathlength mismatch, Δ_{nL}, needed to suppress second-order distortion. The required amount of Δ_{nL} is determined by the R parameter of the modulator. To use the WIB technique in a practical modulator, we need to have R significantly different from unity so that Δ_{nL} is finite.

The R parameter expresses the nonlinearity of the V_π dependence on wavelength. In the following, we examine this dependence and show how it is determined by the choice of design parameters and materials.

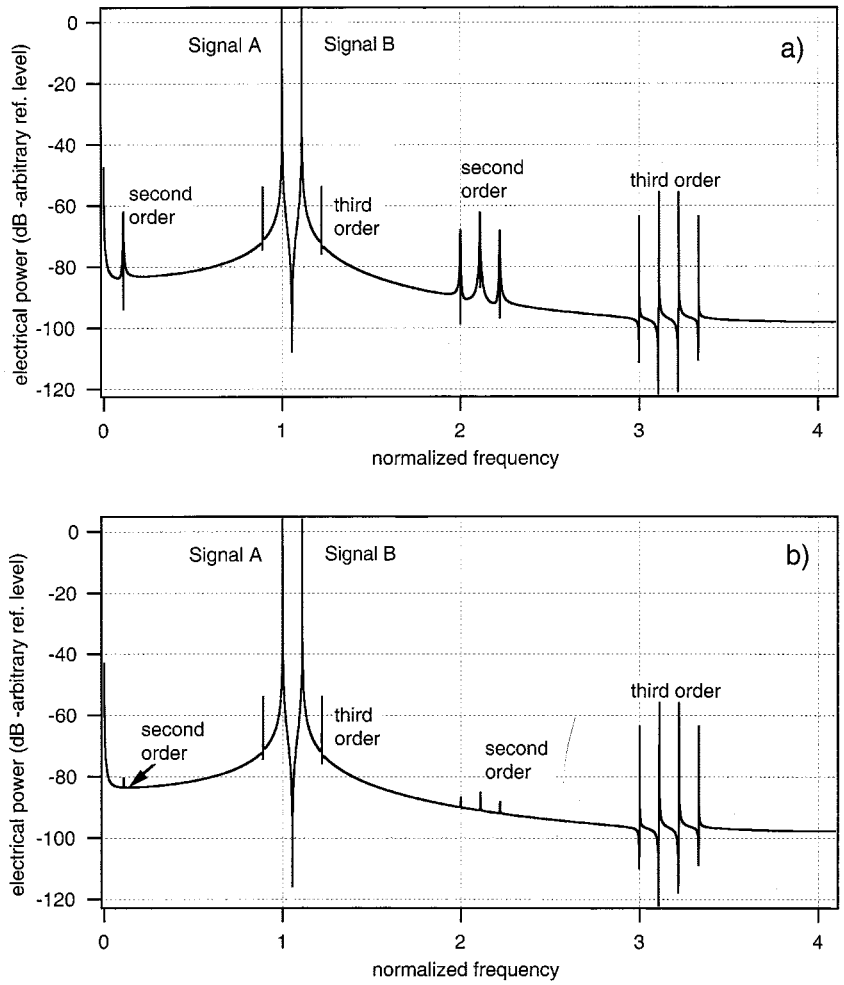

Fig. 4. Spectrum of (a) modulator with an internal bias of $\lambda/4$ and (b) modulator with WIB. $\Delta\lambda = 60$ nm and $m = 0.1$.

By differentiating (1b) with respect to wavelength, we get the following derivative:

$$\frac{dV_\pi}{d\lambda} = \frac{V_\pi}{\lambda}\left[1 - \lambda\left(3\,\frac{dn/d\lambda}{n} + \frac{dr/d\lambda}{r} + \frac{d\Gamma/d\lambda}{\Gamma}\right)\right] \quad (20)$$

and therefore

$$R = \left.\frac{dV_\pi}{d\lambda}\right|_{\lambda o} \Big/ \frac{V_{\pi o}}{\lambda_o} = \left[1 - \left(3\,\frac{dn/d\lambda}{n/\lambda} + \frac{dr/d\lambda}{r/\lambda} + \frac{d\Gamma/d\lambda}{\Gamma/\lambda}\right)\right|_{\lambda o}\Bigg]. \quad (21)$$

For a polymer modulator, our measurements indicate

$$R_n \equiv \frac{(dn/d\lambda)|_{\lambda o}}{n_o/\lambda_o} = \frac{-0.02\ \mu\text{m}^{-1}}{(1.59/1.55)\,\mu\text{m}^{-1}} = -0.024$$

is the index wavelength dependence nonlinearity

$$R_r \equiv \frac{(dr/d\lambda)|_{\lambda o}}{r_o/\lambda_o} = \frac{-26\,(\text{pm/V}/\mu\text{m})}{54/1.55\,(\text{pm/V}/\mu\text{m})} = -0.75$$

is the r_{33} wavelength dependence nonlinearity

$$R_\Gamma \equiv \frac{(d\Gamma/d\lambda)|_{\lambda o}}{\Gamma/\lambda_o} = \frac{\Delta\Gamma}{\Gamma_o} \Big/ \frac{\Delta\lambda}{\lambda_o} = -0.07$$

is the fill factor wavelength dependence nonlinearity.

TABLE I
VALUES FOR R AND ITS CONSTITUENT COMPONENTS FOR THREE MODULATORS

	USC polymer	Sumitomo	Poudyal & Mezhoudi
R_n (μm^{-1})	-0.020	N/A	-0.031
R_r (μm^{-1})	-0.746	N/A	0
R_Γ (μm^{-1})	-0.072	N/A	-0.95
R calculated	1.9	N/A	2.04
R measured	2.2	1.88	2.45

The above evaluation shows that the USC polymer modulator [7] R value is dominated by the nonlinearity of the r coefficient with wavelength and, therefore, can be tailored by the choice of materials. The unusually low wavelength dependence of the confinement factor occurs because in our design even as the mode expands, its overlap with the applied electric field changes very little. Using the above R values in (21), we get $R = 1.9$, which is close to the measured value of 2.2; see Table I.

It is interesting to compare the polymer modulator R value to that of lithium niobate. Table I shows the available relevant values for polymer and two $LiNbO_3$ modulators. The wavelength dependence of $LiNbO_3$ modulators is dominated by the

wavelength variation of the confinement factor, R_Γ, and therefore can be tailored by the waveguide design. It is worth noting that for all modulators in Table I, the R coefficient is around 2.

The key to WIB technique implementation is a modulator with a predetermined internal modulator pathlength mismatch, Δ_{nLo}, and therefore, it is important to consider the tolerance placed on Δ_{nLo}.

The desired internal modulator pathlength mismatch is calculated from the measured value of R for a given modulator design using (19), but the actual value, $\Delta_{nLo}^{(act)}$, may be different due to manufacturing errors

$$\delta \equiv \Delta_{nLo}^{(act)} - \Delta_{nLo}. \tag{22}$$

The bias voltage however is experimentally set to bias the modulator in quadrature irrespective of what the $\Delta_{nLo}^{(act)}$ is. Under these conditions, the effect of the internal pathlength mismatch error is to violate the condition of (15) and create a finite $(d\phi_b/d\lambda)|_{\lambda_o}$ resulting in a finite $\Delta\phi_b$, (8). Using (10), which defines the maximum allowable $\Delta\phi_b$ beyond which the SFDR begins to degrade due to second-order distortion, the allowable pathlength mismatch error for a given wavelength sweep and SFDR is given by

$$\delta = \frac{2\sqrt{6}}{\pi}\,\frac{1}{R}\,\frac{\lambda_o}{\Delta\lambda}\,10^{-(\mathrm{SFDR}_3/40)}\Delta_{nLo}. \tag{23}$$

For a wavelength sweep of $\Delta\lambda = 60$ nm, at $\lambda_o = 1550$ nm, $\mathrm{SFDR}_3 = 80$ dB, and assuming a typical $R = 2$ the tolerance on Δ_{nLo} is $\delta/\Delta_{nLo} = 0.2$. A 20% tolerance on the internal pathlength mismatch should be well within manufacturing tolerances.

VI. Conclusion

The optical bandwidth of RF photonic systems and photonic assisted A/D systems which use a single MZ modulator and have greater than one octave RF bandwidth is restricted by the second-order distortion caused by the MZ modulator. Such systems have been analyzed to determine the relation between the optical bandwidth and SFDR. For systems with a noise floor set by third-order distortion to a SFDR of 80 dB, the allowable optical bandwidth is limited to 24 nm, in the 1550-nm band. The cause of the increased second-order distortion is the change in the bias point of the modulator as the wavelength varies. We propose a novel WIB technique that relies on proper combination of interferometer pathlength imbalance and applied bias trim voltage to reduce the changes in bias point with wavelength. Using the WIB design for a typical polymer based modulator, the second-order distortion can be decreased by 24 dB.

Acknowledgment

The authors would like to thank Dr. S. Pappert for helpful discussions.

References

[1] V. Poudyal and M. Mezhoudi, "Simultaneous modulation of multiple optical channels with a single Ti : LiNbO3 Mach–Zehnder modulator in a WDM system," in *ICT '98 Int. Conf. Telecommunications*, 1998, pp. 72–76.

[2] F. Coppinger, A. S. Bhushan, and B. Jalali, "Photonic time stretch and its applications to analog-to-digital conversion," *IEEE Trans. Microwave Theory Tech.*, vol. 47, pp. 1309–1314, July 1999.

[3] M. C. Nuss, W. H. Knox, and U. Koren, "Scalable 32 channel chirped-pulse WDM source," *Electron. Lett.*, vol. 32, no. 14, pp. 1311–1312, 1996.

[4] B. H. Kolner and D. W. Dolfi, "Intermodulation distortion and compression in an integrated electrooptic modulator," *Appl. Opt.*, vol. 26, no. 17, pp. 3676–3680, 1987.

[5] V. Poudyal and M. Mezhoudi, "Wavelength sensitivity of Ti : LiNbO3 Mach–Zehnder interferometer," *Proc. SPIE*, vol. 2291, pp. 196–207, 1994.

[6] "Sumitomo MZ modulator TMZ-10 data sheet. V_π changes from 6.5 V to 6.7 V over 25 nm,".

[7] H. Zhang, M.-C. Oh, A. Szep, W. H. Steier, C. Zhang, L. R. Dalton, H. Erlig, Y. Chang, D. H. Chang, and H. R. Fetterman, "Push pull electro-optic polymer modulators with low half-wave voltage and low loss at both 1310 nm and 1550 nm," *Appl. Phys. Lett.*, vol. 78, pp. 3116–3118, 2001.

D. Dubovitsky (S'93–M'95), photograph and biography not available at the time of publication.

W. H. Steier (S'58–M'60–SM'72–F'76–LF'97), photograph and biography not available at the time of publication.

S. Yegnanarayanan, photograph and biography not available at the time of publication.

B. Jalali (S'86–M'89–SM'97), photograph and biography not available at the time of publication.